

Measurement of the associated production of a Higgs boson decaying into b-quarks with a vector boson at high transverse momentum with the ATLAS detector



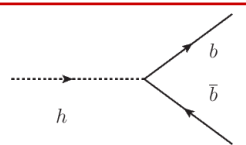
Maria Giovanna Foti
on behalf of the ATLAS Collaboration



Epiphany 2021, XXVII Cracow Epiphany Conference on Future of particle physics
7th-10th January 2021

Physics motivations

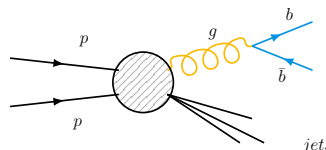
H(bb)



Largest BR in SM (~58%)

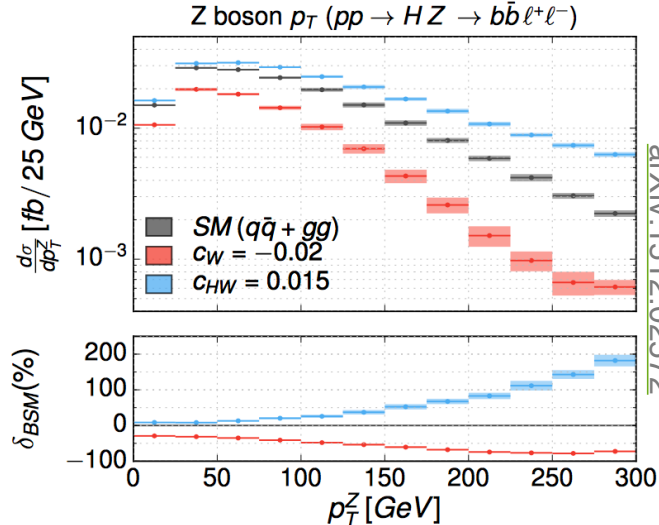
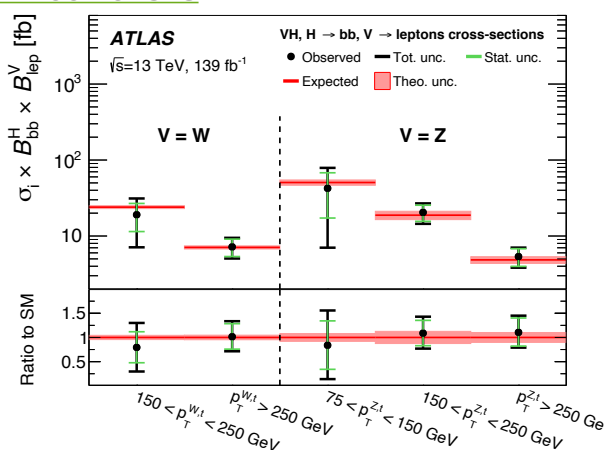
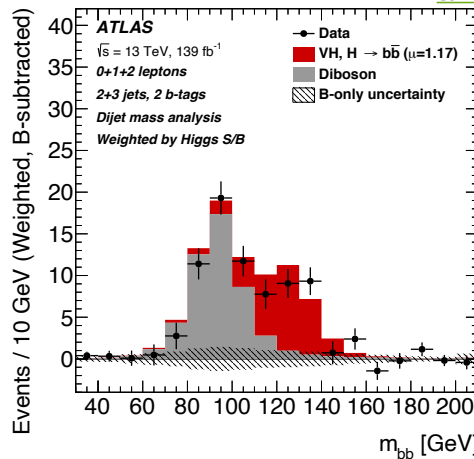
Measurement of Yukawa coupling to down-type quarks

Challenge to H(bb): large multi-jet background



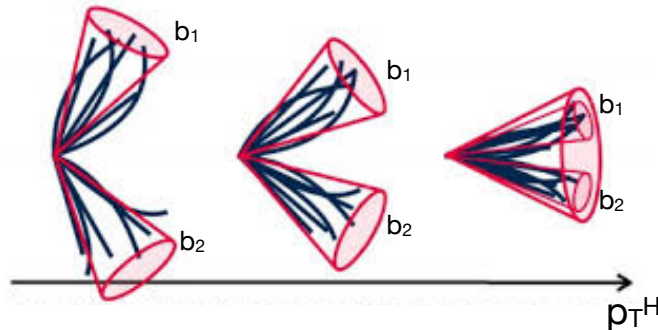
Study VH production ($V=W,Z$), **$V \rightarrow$ leptons**: distinctive signature, efficient trigger and large reduction of multi-jet events

arXiv:2007.02873



- ▶ In search for new physics, BSM scenarios often predict **deviations from the SM at high p_T**
 - Need to have a more detailed view at this energy regime

Strategy and event selection



$$\Delta R(b_1, b_2) \approx \frac{2 \cdot m_H}{p_T^H}$$

$$\underline{\Delta R(b_1, b_2) \leq 1, \quad p_T^H \geq 250 \text{ GeV}}$$

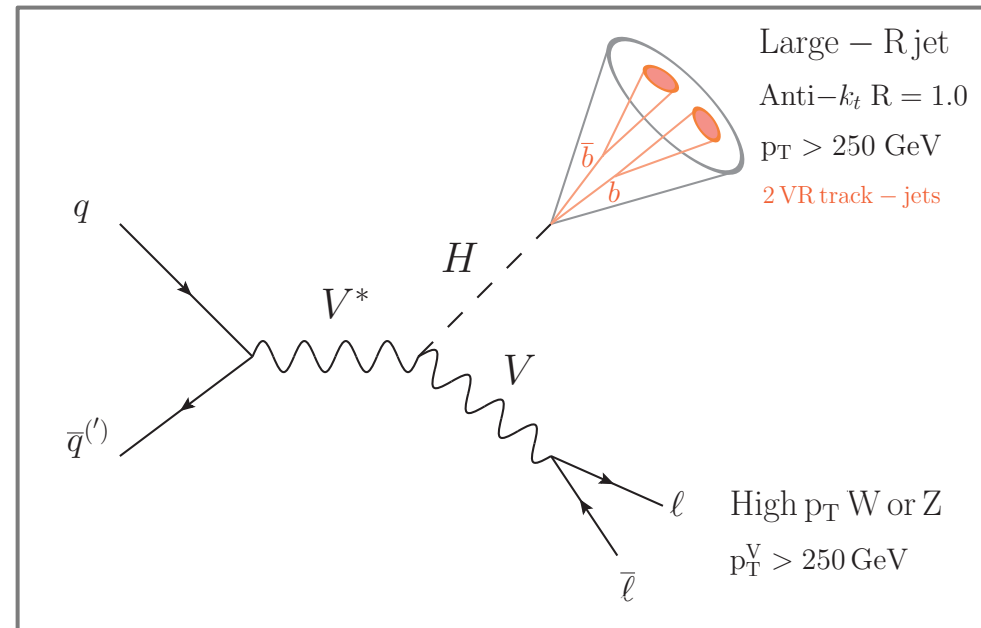
Higgs candidate:

[arXiv:2008.02508](https://arxiv.org/abs/2008.02508)

- Large-radius (R) calorimeter jet (trimmed anti- k_t R=1.0), $p_T > 250 \text{ GeV}$
- ≥ 2 variable-radius (VR) track jets matched to Large-R jet
- Leading 2 VR track jets b-tagged (MV2c10@70%)

Number of charged leptons ($\ell = e, \mu$) in leptonic V decay determines analysis channel:

- $Z \rightarrow \nu\nu$ (0L)
- $W \rightarrow \ell\nu$ (1L)
- $Z \rightarrow \ell\ell$ (2L)

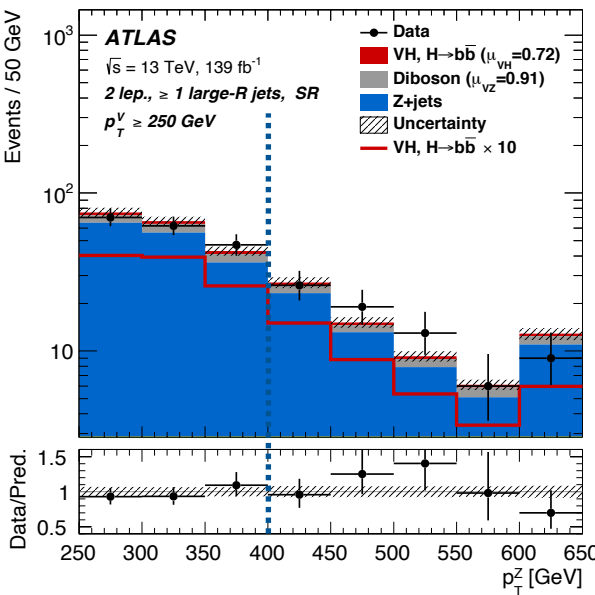


Event categorisation

[arXiv:2008.02508](https://arxiv.org/abs/2008.02508)

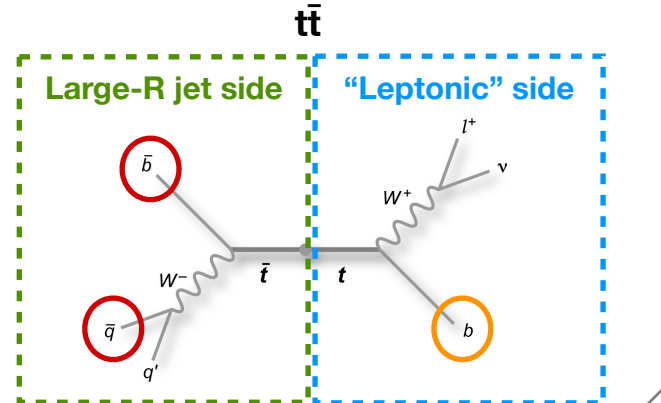
Additional categorisation for 0L and 1L

PTV



p_T^V bins: 250-400 GeV and
> 400 GeV

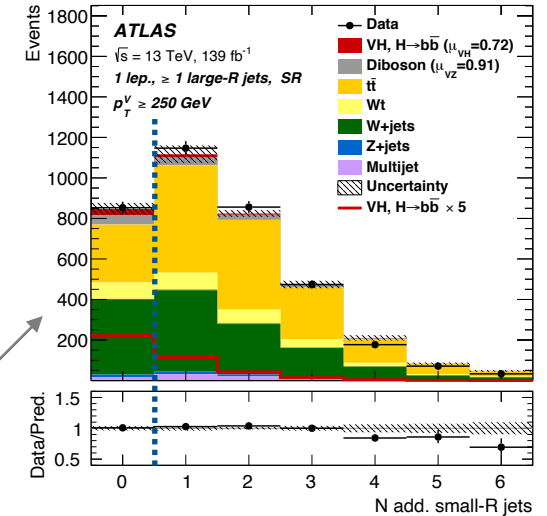
Signal and Control Regions



- ▶ **SR** - signal-enriched region:
 - 2 **signal b-jets**: b-tagged track jets **associated to Large-R jet**
 - 0 **additional b-jets**: no b-tagged track jets **not associated to Large-R jet**

- ▶ **Top CR** - top-enriched region:
 - 2 **signal b-jets**: b-tagged track jets **associated to Large-R jet**
 - 1+ **additional b-jets**: 1+ b-tagged track jets **not associated to Large-R jet**

High and Low Purity Signal Regions



SR further divided into high (HP) and low (LP) purity categories:

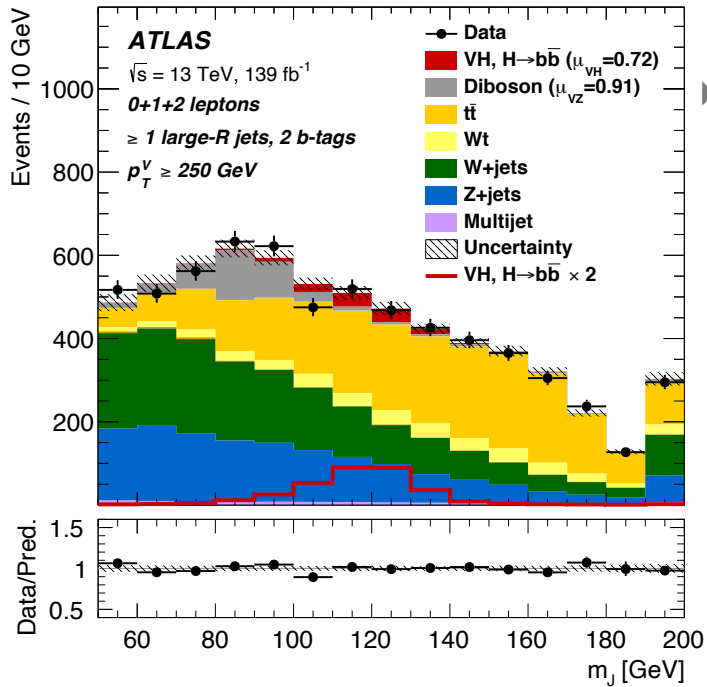
► High Purity SR:

- **0 additional calo-jets:** Small-R ($R=0.4$) calorimeter-jets not associated to Large-R jet

► Low Purity SR:

- **1+ additional calo-jets:** Small-R ($R=0.4$) calorimeter-jets not associated to Large-R jet

Background processes and fit model



Background modelling strategy:

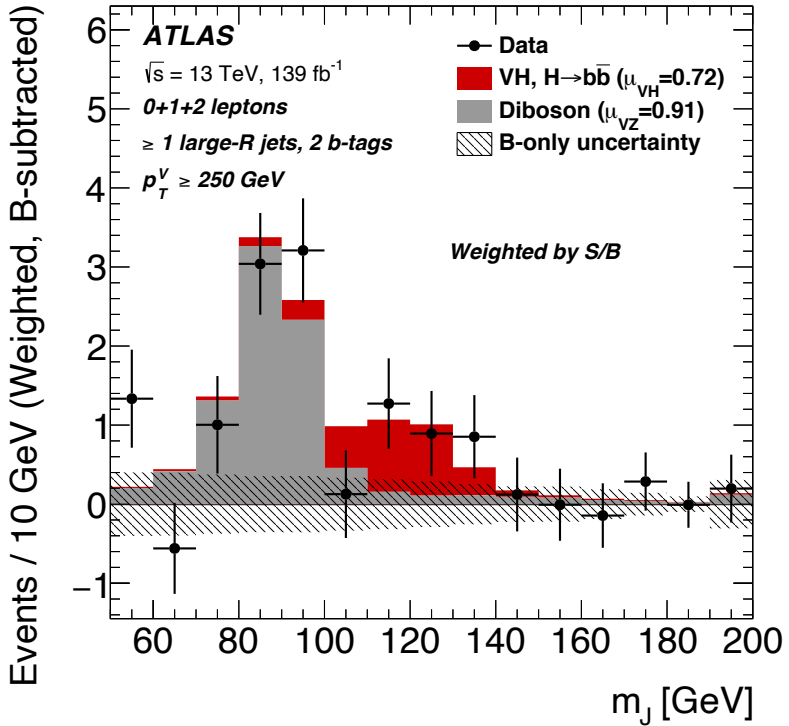
- $t\bar{t}$, $W+hf$, $Z+hf$, Diboson: dominant backgrounds, templates extracted from simulation, normalisation from data
- Single top, V+light flavours (ll, cl)*: template and normalisation uncertainties from simulation
- Multi-jet: suppressed with dedicated cuts, residual contribution studied in data

*< 5% of total V+jets

- ▶ Signal extracted using binned profile likelihood fit with Large-R jet mass (m_j) as discriminant
 - Fit 10 signal and 4 control regions simultaneously
- ▶ Simultaneous measurement of signal strength parameters μ_{VH} and μ_{VZ} :

$$\mu = \frac{\sigma_{meas}}{\sigma_{SM}}$$

Results



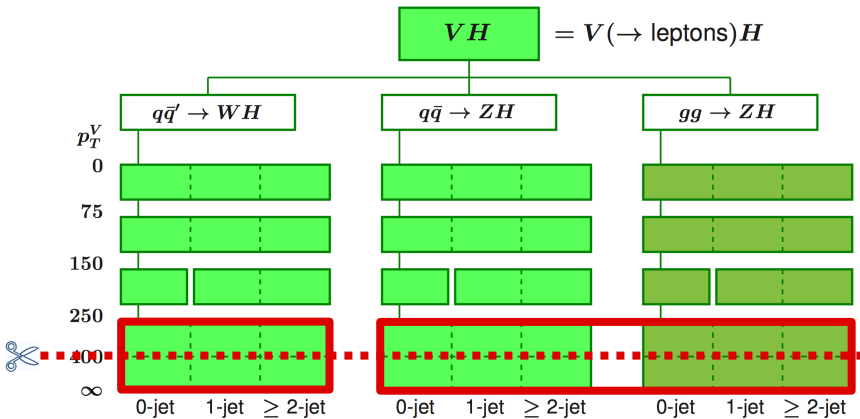
| Measurement | Expected sig. | Observed sig. |
|-------------|---------------|---------------|
| 0L | 1.86 | 1.43 |
| 1L | 1.96 | 1.95 |
| 2L | 1.24 | -0.13 |
| WH | 1.92 | 2.04 |
| ZH | 1.79 | 0.63 |
| combined | 2.73 | 2.05 |

$$\mu_{VH}^{bb} = 0.72^{+0.39}_{-0.36} = 0.72^{+0.29}_{-0.28} (\text{stat.})^{+0.26}_{-0.22} (\text{syst.}) \quad \sigma_{VH}^{bb} = 2.1 (2.7) \text{ obs. (exp.)}$$

$$\mu_{VZ}^{bb} = 0.91^{+0.29}_{-0.23} = 0.91 \pm 0.15 (\text{stat.})^{+0.25}_{-0.17} (\text{syst.}) \quad \sigma_{VZ}^{bb} = 5.4 (5.7) \text{ obs. (exp.)}$$

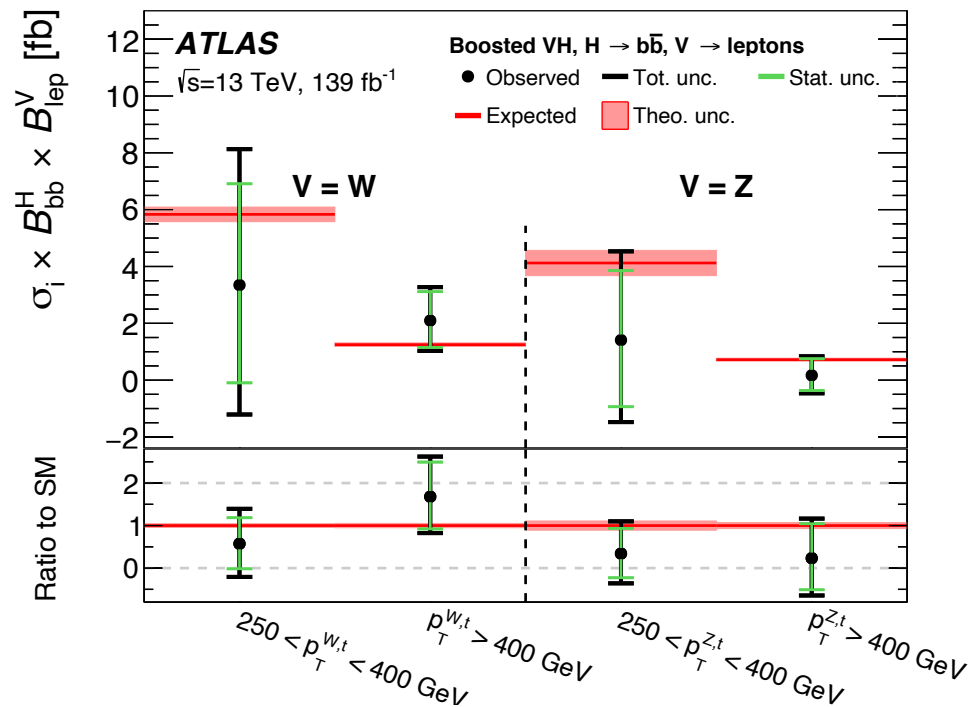
Simplified Template Cross Section (STXS)

- ▶ Differential cross section measurement in “simplified” fiducial regions
- ▶ STXS measurement in 2 p_T^V analysis bins: $[250, 400[$, $[400, \infty[$



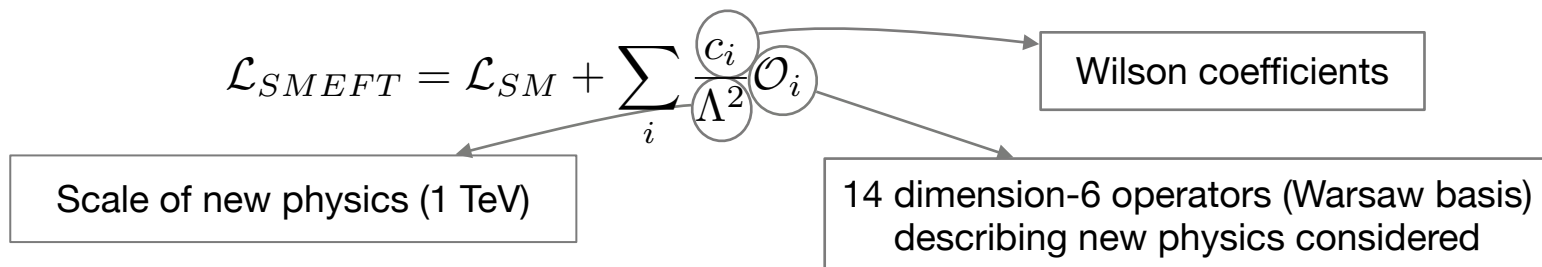
[arXiv:1906.02754](#)

| Measurement | Expected sig. | Observed sig. |
|--------------------------|---------------|---------------|
| WH $[250, 400]$ GeV | 1.26 | 0.73 |
| WH $[400, \infty]$ GeV | 1.27 | 2.02 |
| ZH $[250, 400]$ GeV | 1.38 | 0.49 |
| ZH $[400, \infty]$ GeV | 1.12 | 0.26 |



Effective Field Theory (EFT) interpretation

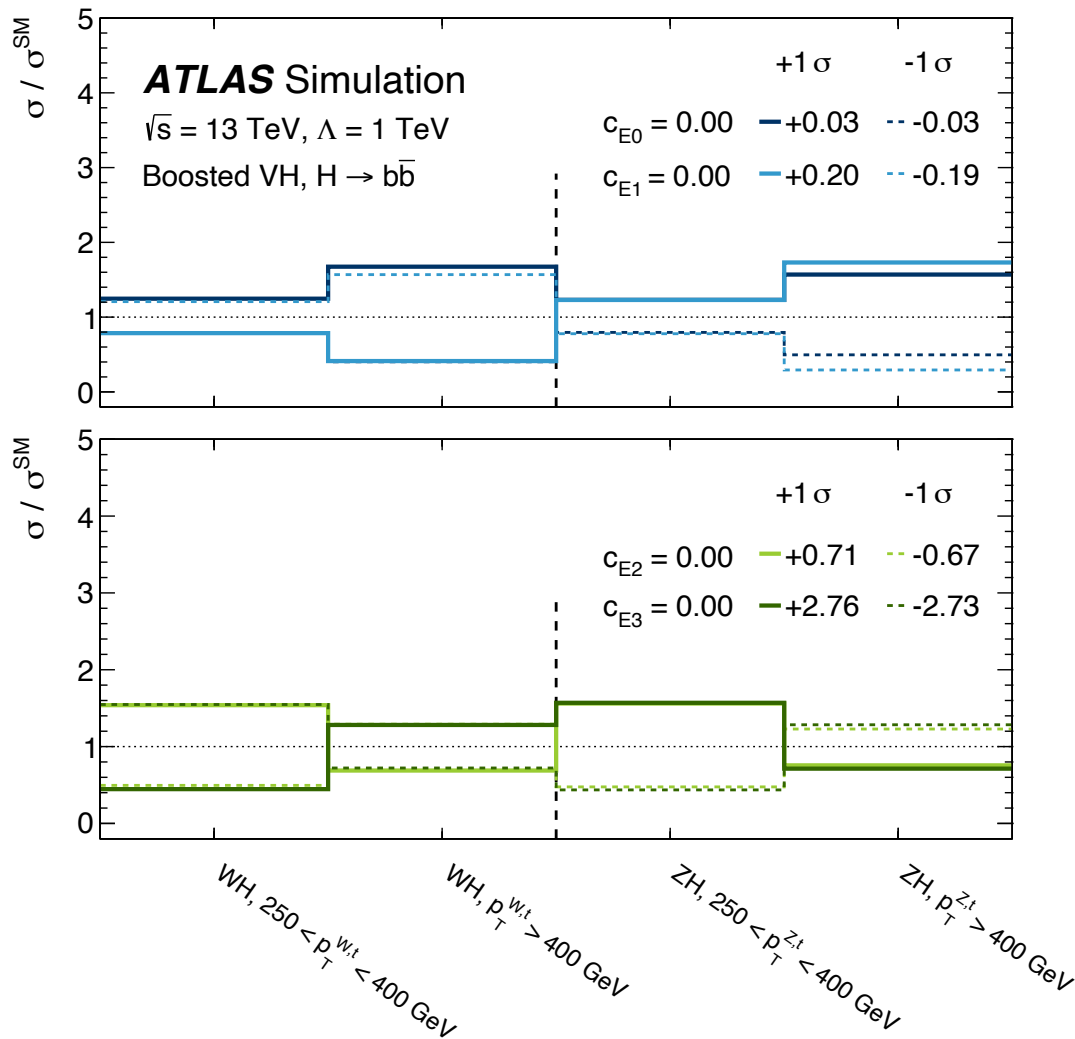
- Model-independent way to test presence of BSM physics
- Parameterisation of BSM effects using effective Lagrangian operators in Warsaw basis.



- Parametrise $\sigma(qq \rightarrow ZH)$, $\sigma(qq \rightarrow WH)$, $BR(H \rightarrow bb)$ as linear/quadratic polynomials in c_i
- Extract 95% CL limits for leading c_i coefficients

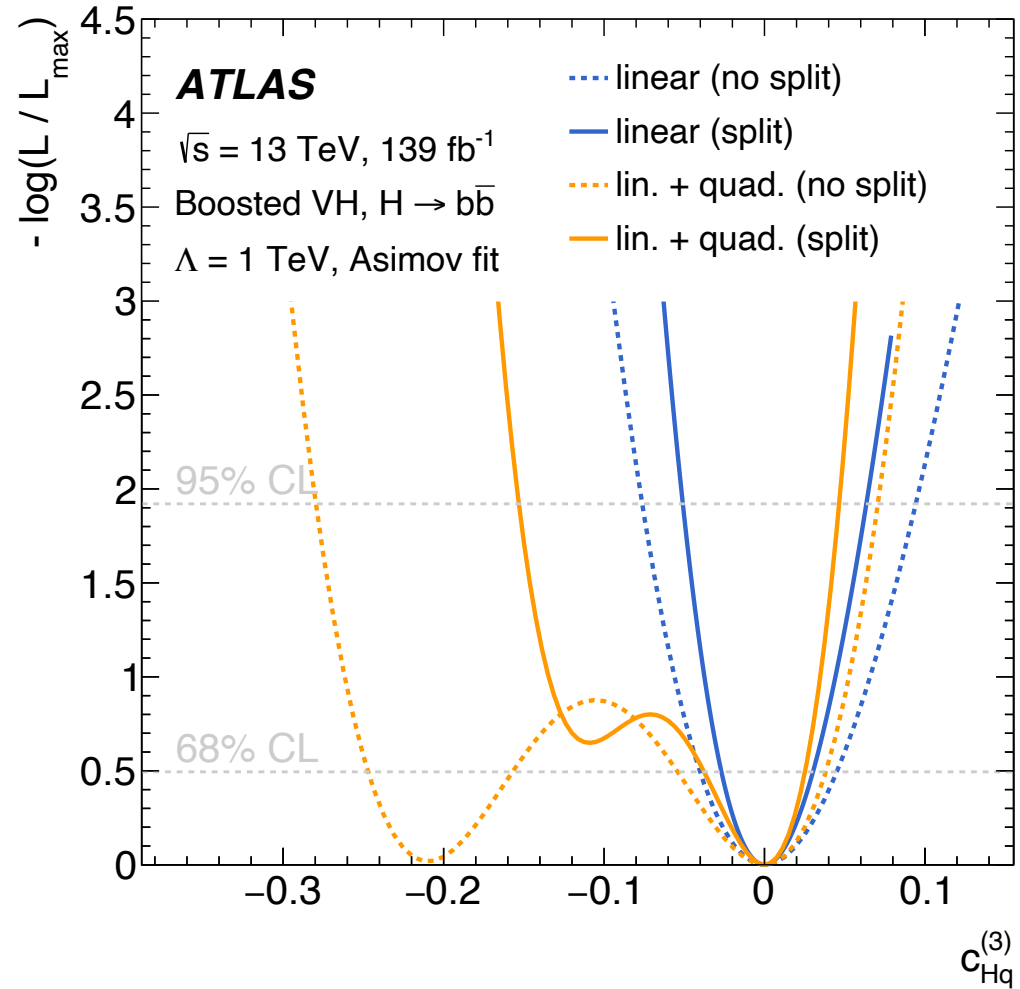
| Coefficient | Operator |
|----------------|--|
| c_H | $(H^\dagger H)(H^\dagger H)$ |
| c_{HDD} | $(H^\dagger D^\mu H)^*(H^\dagger D_\mu H)$ |
| $ c_{dH} $ | $(H^\dagger H)(\bar{q}_p d_r H)$ |
| c_{HW} | $H^\dagger HW_{\mu\nu}^I W^{I\mu\nu}$ |
| c_{HB} | $H^\dagger HB_{\mu\nu} B^{\mu\nu}$ |
| c_{HWB} | $H^\dagger \tau^I HW_{\mu\nu}^I B^{\mu\nu}$ |
| $c_{Hl}^{(1)}$ | $H^\dagger i \overleftrightarrow{D}_\mu H (\bar{l}_p \gamma^\mu l_r)$ |
| $c_{Hl}^{(3)}$ | $H^\dagger i \overleftrightarrow{D}_\mu^I H (\bar{l}_p \tau^I \gamma^\mu l_r)$ |
| $c_{He}^{(1)}$ | $H^\dagger i \overleftrightarrow{D}_\mu H (\bar{e}_p \gamma^\mu e_r)$ |
| $c_{Hq}^{(1)}$ | $H^\dagger i \overleftrightarrow{D}_\mu H (\bar{q}_p \gamma^\mu q_r)$ |
| $c_{Hq}^{(3)}$ | $H^\dagger i \overleftrightarrow{D}_\mu^I H (\bar{q}_p \tau^I \gamma^\mu q_r)$ |
| c_{Hu} | $H^\dagger i \overleftrightarrow{D}_\mu H (\bar{u}_p \gamma^\mu u_r)$ |
| c_{Hd} | $H^\dagger i \overleftrightarrow{D}_\mu H (\bar{d}_p \gamma^\mu d_r)$ |
| $c_{ll}^{(1)}$ | $(\bar{l}_p \gamma_\mu l_r)(\bar{l}_s \gamma^\mu l_t)$ |

EFT results



- ▶ Effect of $\pm 1\sigma$ variation of the **four independent deformations to the SM** the analysis can identify, based on the measurement of STXS bins

Effect of dedicated bin above 400 GeV



Conclusions

- ▶ First VH(bb) analysis at high- p_T ($p_T^V > 250$ GeV), using boosted techniques:

$$\mu_{VH}^{bb} = 0.72^{+0.39}_{-0.36} = 0.72^{+0.29}_{-0.28}(\text{stat.})^{+0.26}_{-0.22}(\text{syst.})$$

$$\mu_{VZ}^{bb} = 0.91^{+0.29}_{-0.23} = 0.91 \pm 0.15(\text{stat.})^{+0.25}_{-0.17}(\text{syst.})$$

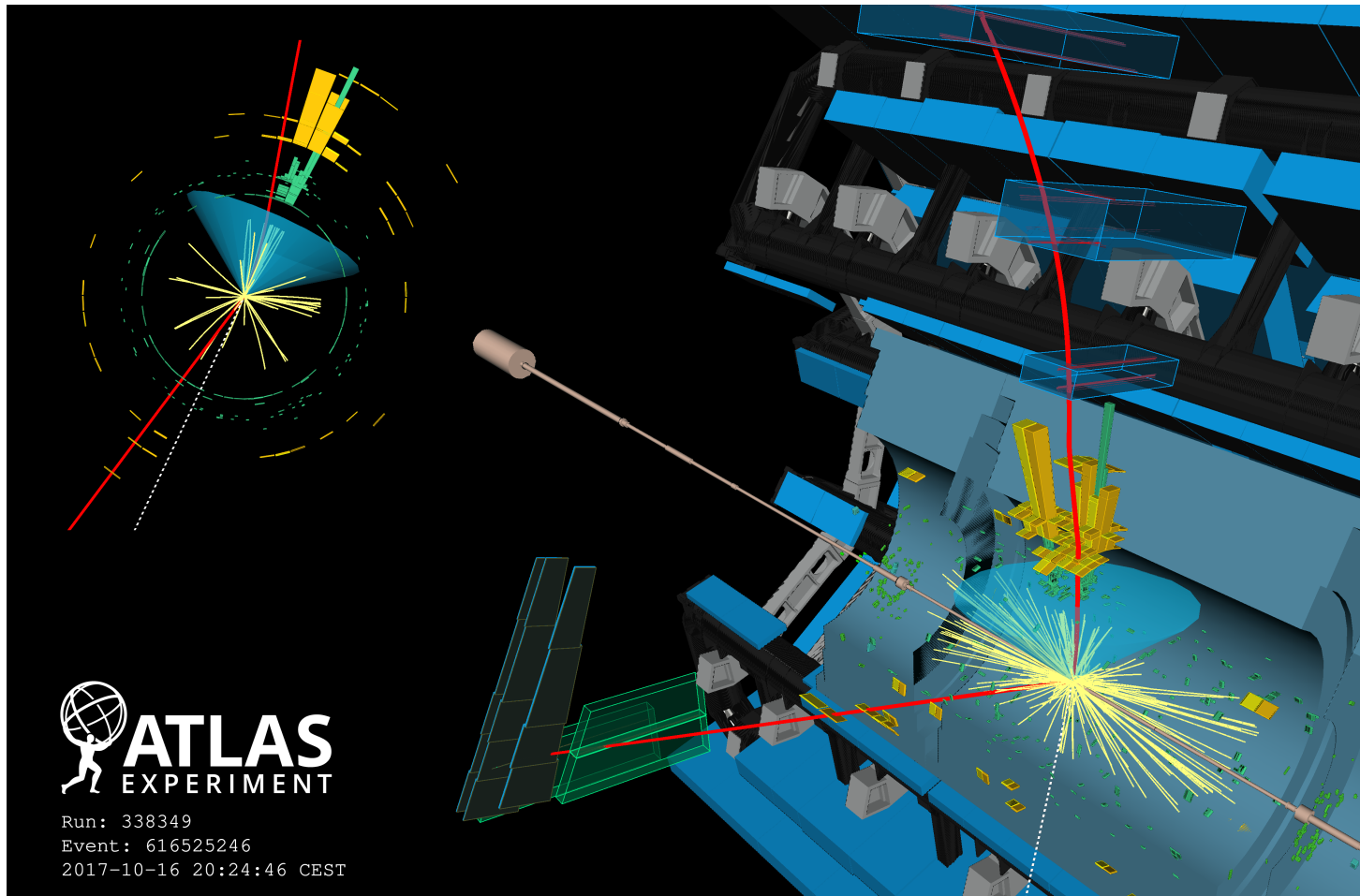
- ▶ Measurement is in agreement with the SM expectations

$$\sigma_{VH}^{bb} = 2.1 (2.7) \text{ obs. (exp.)}$$

$$\sigma_{VZ}^{bb} = 5.4 (5.7) \text{ obs. (exp.)}$$

- ▶ First STXS measurement of $p_T(V, \text{truth}) > 400$ GeV, well in agreement with SM prediction
- ▶ Provided EFT interpretation of the results

Thank you!



[arXiv:2008.02508](#)

CERN Physics briefing: [link](#)

Backup

Event selection details

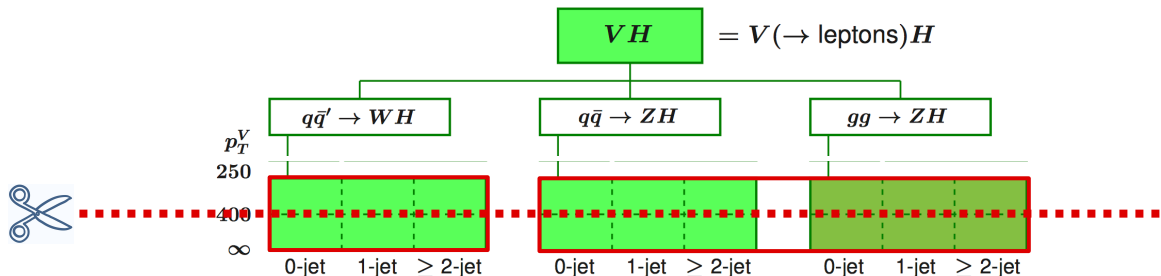
| Selection | 0 lepton channel | 1 lepton channel | | 2 leptons channel | |
|--|---------------------------|---|---------------------------|---|---------------------|
| | | e sub-channel | μ sub-channel | e sub-channel | μ sub-channel |
| Trigger | E_T^{miss} | Single electron | E_T^{miss} | Single electron | E_T^{miss} |
| Leptons | 0 <i>baseline</i> leptons | 1 <i>signal</i> lepton $p_T > 27 \text{ GeV}$ $p_T > 25 \text{ GeV}$ no second <i>baseline</i> lepton | | 2 <i>baseline</i> leptons among which ≥ 1 <i>signal</i> lepton, $p_T > 27 \text{ GeV}$ both leptons of the same flavour - | opposite sign muons |
| E_T^{miss} | $> 250 \text{ GeV}$ | $> 50 \text{ GeV}$ | - | | - |
| p_T^V | | | $p_T^V > 250 \text{ GeV}$ | | |
| Large- R jets | | at least one large- R jet, $p_T > 250 \text{ GeV}$, $ \eta < 2.0$ | | | |
| Track-jets | | at least two track-jets, $p_T > 10 \text{ GeV}$, $ \eta < 2.5$, matched to the leading large- R jet | | | |
| b -jets | | leading two track-jets matched to the leading large- R must be b -tagged (MV2c10, 70%) | | | |
| m_J | | $> 50 \text{ GeV}$ | | | |
| $\min[\Delta\phi(\vec{E}_T^{\text{miss}}, \text{small-}R \text{ jets})]$ | $> 30^\circ$ | - | | | |
| $\Delta\phi(\vec{E}_T^{\text{miss}}, H_{\text{cand}})$ | $> 120^\circ$ | - | | | |
| $\Delta\phi(\vec{E}_T^{\text{miss}}, E_{T, \text{trk}}^{\text{miss}})$ | $< 90^\circ$ | - | | | |
| $\Delta y(V, H_{\text{cand}})$ | - | $ \Delta y(V, H_{\text{cand}}) < 1.4$ | | | |
| $m_{\ell\ell}$ | | - | | $66 \text{ GeV} < m_{\ell\ell} < 116 \text{ GeV}$ | |
| Lepton p_T imbalance | | - | | $(p_T^{\ell_1} - p_T^{\ell_2})/p_T^Z < 0.8$ | |

Event categorisation details

| Channel | Categories | | | | | |
|----------|---------------------------------|----------------------------------|----------------------------------|------------------------------|----------------------------------|----------------------------------|
| | $250 < p_T^V < 400 \text{ GeV}$ | | | $p_T^V \geq 400 \text{ GeV}$ | | |
| | 0 add. b -track-jets | | ≥ 1 add. b -track-jets | 0 add. b -track-jets | | ≥ 1 add. b -track-jets |
| | 0 add. small- R jets | ≥ 1 add. small- R jets | | 0 add. small- R jets | ≥ 1 add. small- R jets | |
| 0-lepton | HP SR | LP SR | CR | HP SR | LP SR | CR |
| 1-lepton | HP SR | LP SR | CR | HP SR | LP SR | CR |
| 2-lepton | SR | | | SR | | |

Fit main features

- ▶ **Normalisation of three dominant bkgds are floated:**
 - ttbar → from CR
 - V+hf: W+hf, Z+hf → from sidebands in the SRs.
- ▶ **Systematics:**
 - **Full set of detector systematics:**
 - ▶ **Large-R jets** (p_T , mass)x(scale, resolution)
 - ▶ small-R jets, MET, leptons, b-tagging, pile-up, luminosity
 - **Full set of modelling uncertainties**
 - **MC stat.** unc.: includes VZ but excludes VH (1 NP per bin)
- ▶ 2 p_T^V analysis bins (for STXS): [250,400], [400, ∞]

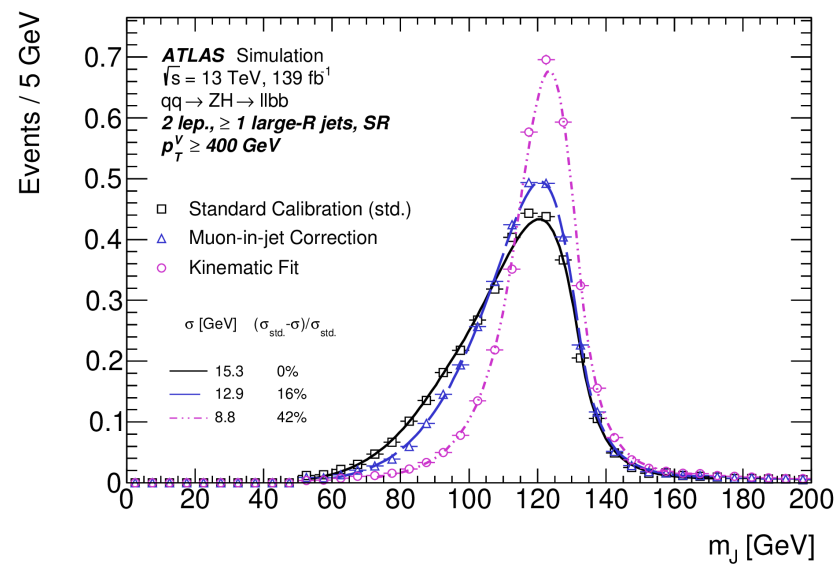
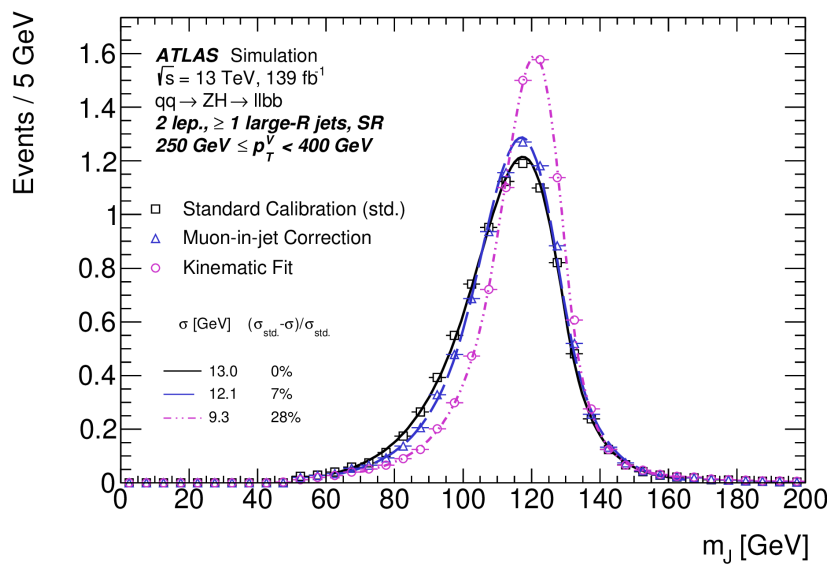


Breakdown of the uncertainties

| Source of uncertainty | Avg. impact | |
|---|--------------------|-------|
| Total | 0.372 | |
| Statistical | 0.283 | |
| Systematic | 0.240 | |
| Experimental uncertainties | | |
| Small- R jets | 0.038 | |
| Large- R jets | 0.133 | |
| E_T^{miss} | 0.007 | |
| Leptons | 0.010 | |
| b -tagging | b -jets | 0.016 |
| | c -jets | 0.011 |
| | light-flavour jets | 0.008 |
| | extrapolation | 0.004 |
| Pile-up | 0.001 | |
| Luminosity | 0.013 | |
| Theoretical and modelling uncertainties | | |
| Signal | 0.038 | |
| Backgrounds | 0.100 | |
| $\hookrightarrow Z + \text{jets}$ | 0.048 | |
| $\hookrightarrow W + \text{jets}$ | 0.058 | |
| $\hookrightarrow t\bar{t}$ | 0.035 | |
| \hookrightarrow Single top quark | 0.027 | |
| \hookrightarrow Diboson | 0.032 | |
| \hookrightarrow Multijet | 0.009 | |
| MC statistical | 0.092 | |

- ▶ Analysis statistically limited.
- ▶ Systematic uncertainties is of same order as the statistical one. Most relevant sources:
 - **Large-R jets (JMR, then JMS)**
 - **Modelling uncertainties**
 - MC stat.

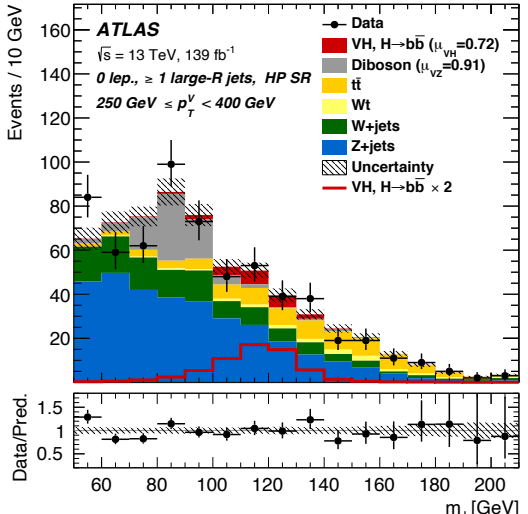
Large-R jet mass



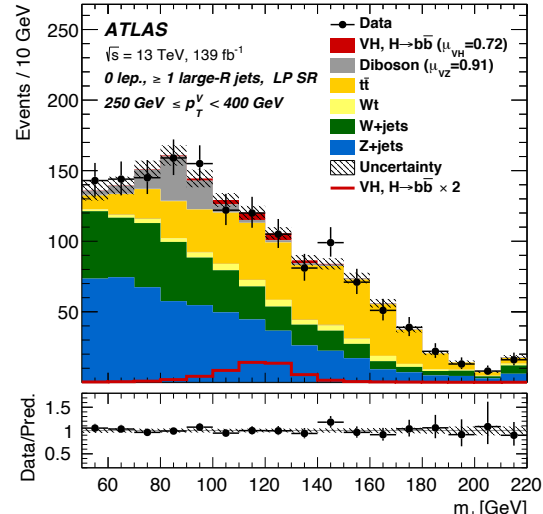
- Final discriminant: Large-R jet mass (m_J). Improve mass resolution on top of calorimeter-based performance using:
 - Combined mass
 - Muon-in-jet-correction
 - Kinematic fit (2L)

Postfit plots: 0L

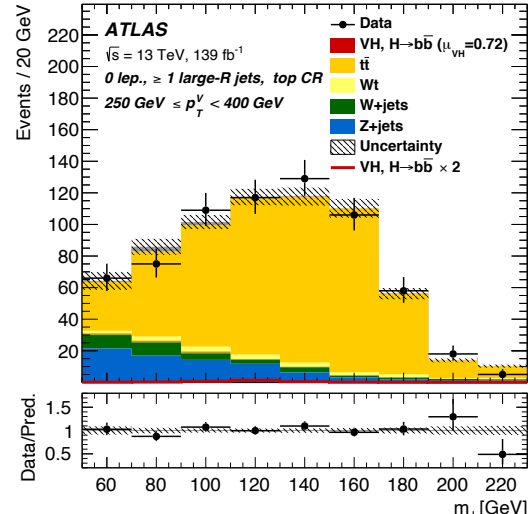
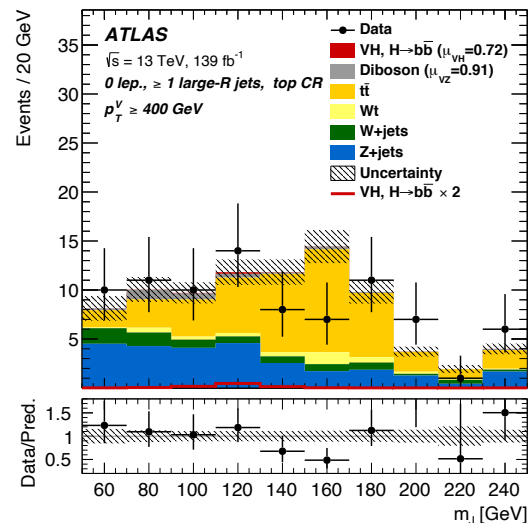
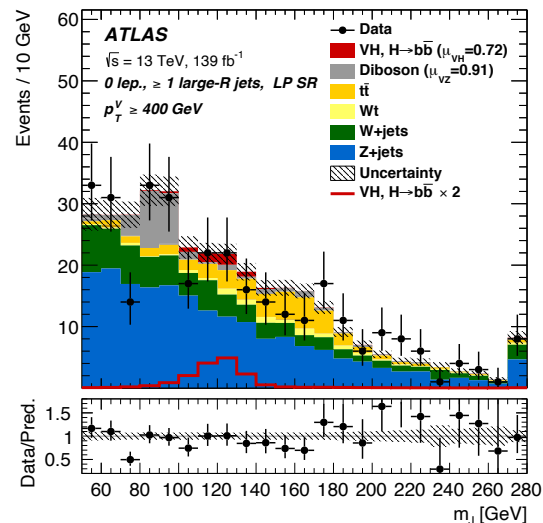
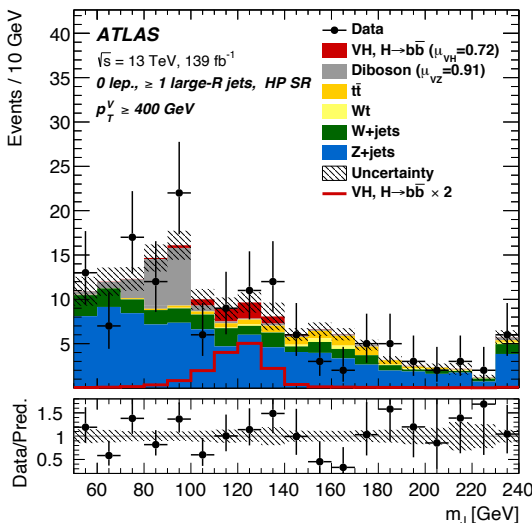
HP SR



LP SR



CR

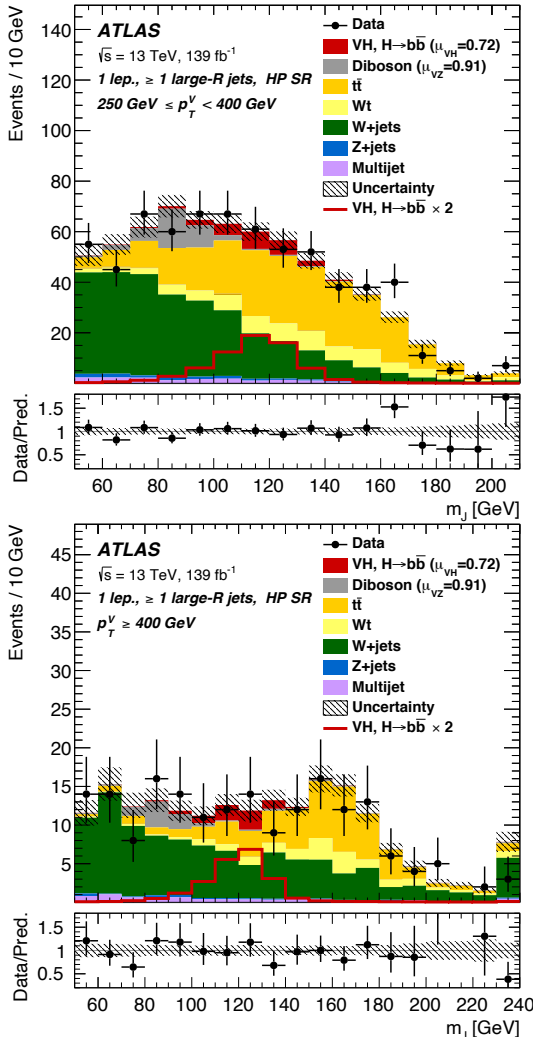
250 GeV < $p_T^V < 400$ GeV

Postfit plots: 1L

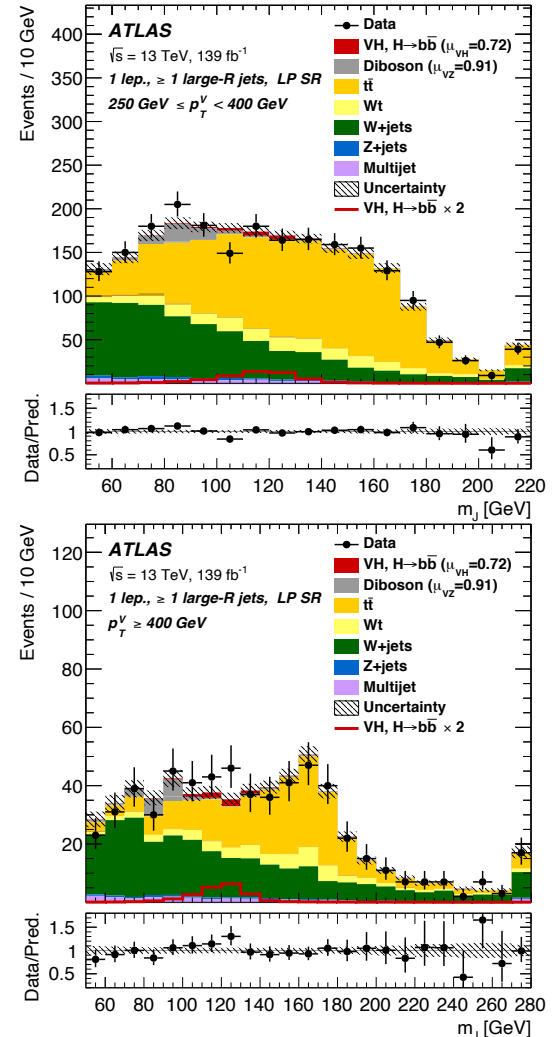
250 GeV < p_T^V < 400 GeV

$p_T^V > 400$ GeV

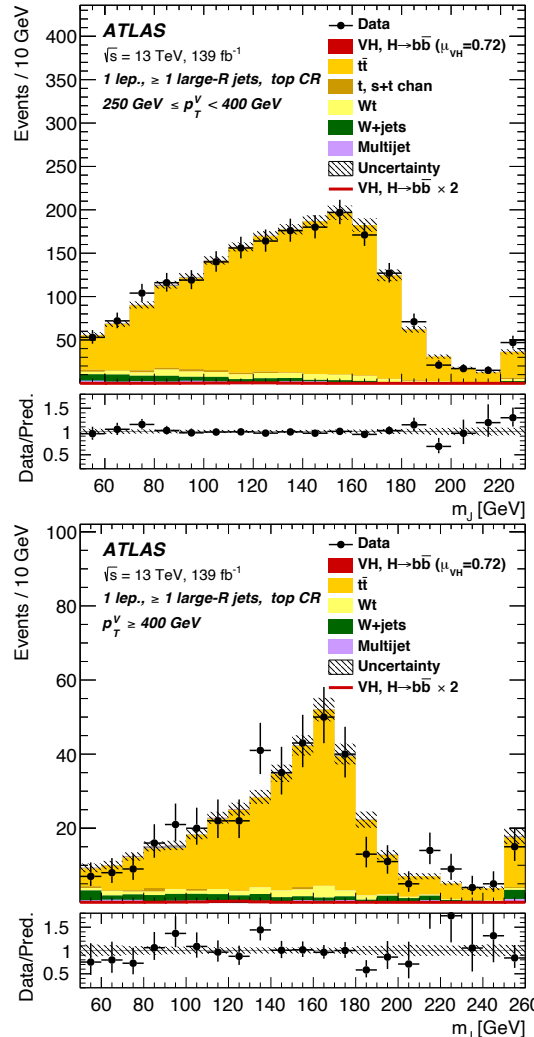
HP SR



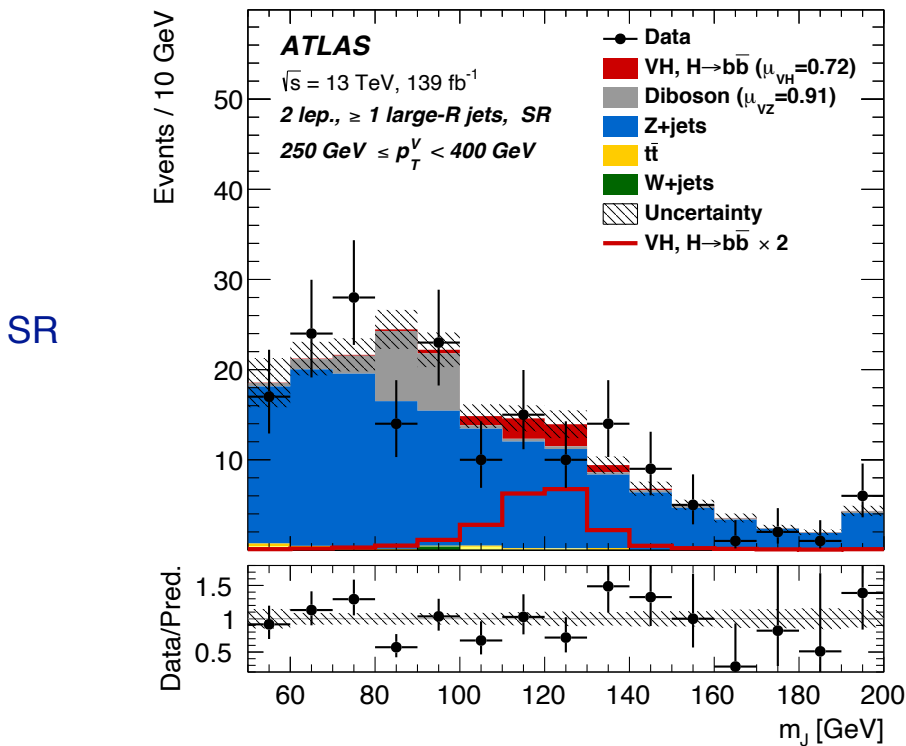
LP SR



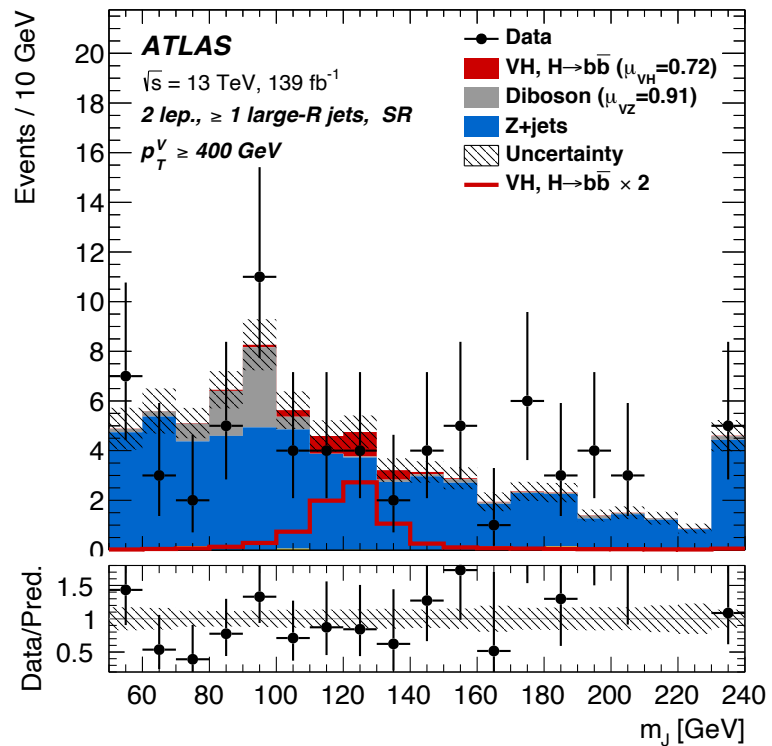
CR



Postfit plots: 2L



$250 \text{ GeV} < p_T^V < 400 \text{ GeV}$



$p_T^V > 400 \text{ GeV}$

Postfit event yields: 0L

| Processes | 250 GeV < p_T^V ≤ 400 GeV | | | p_T^V > 400 GeV | | |
|---------------|-----------------------------|-----------|-------------|-------------------|-----------|---------------|
| | HP SR | LP SR | CR | HP SR | LP SR | CR |
| $W + t$ | 14.7±5.4 | 46±19 | 17.2±8.1 | 2.0±1.0 | 8.93±6.3 | 3.76±2.5 |
| other $t + X$ | 0.79±0.03 | 3.18±0.66 | 4.5±1.3 | - | 0.66±0.03 | 0.1091±0.0041 |
| $t\bar{t}$ | 75±14 | 423±36 | 539±31 | 7.5±1.8 | 38.21±6.8 | 44.07±7.43 |
| VZ | 77±17 | 88±19 | 6.2±1.6 | 17.3±4.1 | 28.77±6.6 | 2.79±0.72 |
| WW | - | 2.15±0.05 | 0.24±0.01 | 0.33±0.02 | 1.80±0.06 | - |
| $W+HF$ | 101±20 | 331±60 | 30±22 | 20.2±6.2 | 59.8±18 | 6.6±5.1 |
| $W + cl$ | 5.1±2.3 | 8.4±3.2 | 0.46±0.01 | 0.99±0.69 | 2.8±1.1 | 0.19±0.07 |
| $W + l$ | 5.6±3.9 | 4.6±2.5 | 0.160±0.003 | 1.4±2.0 | 2.7±1.7 | 0.57±0.36 |
| $Z+HF$ | 319±35 | 549±62 | 77±21 | 87±11 | 185±21 | 25.8±7.4 |
| $Z + cl$ | 4.0±1.6 | 6.7±2.7 | 0.83±0.02 | - | 6.4±2.7 | 0.93±0.41 |
| $Z + l$ | 1.34±0.67 | 3.6±2.1 | 0.42±0.01 | 1.05±0.63 | 3.7±2.5 | 0.29±0.16 |
| Signal | 22±11 | 19.0±9.8 | 1.05±0.54 | 5.7±2.9 | 5.9±3.0 | 0.33±0.17 |
| Background | 603±25 | 1466±36 | 676±25 | 137.6±8.5 | 339±15 | 85.1±7.3 |
| data | 623 | 1493 | 683 | 146 | 330 | 85 |

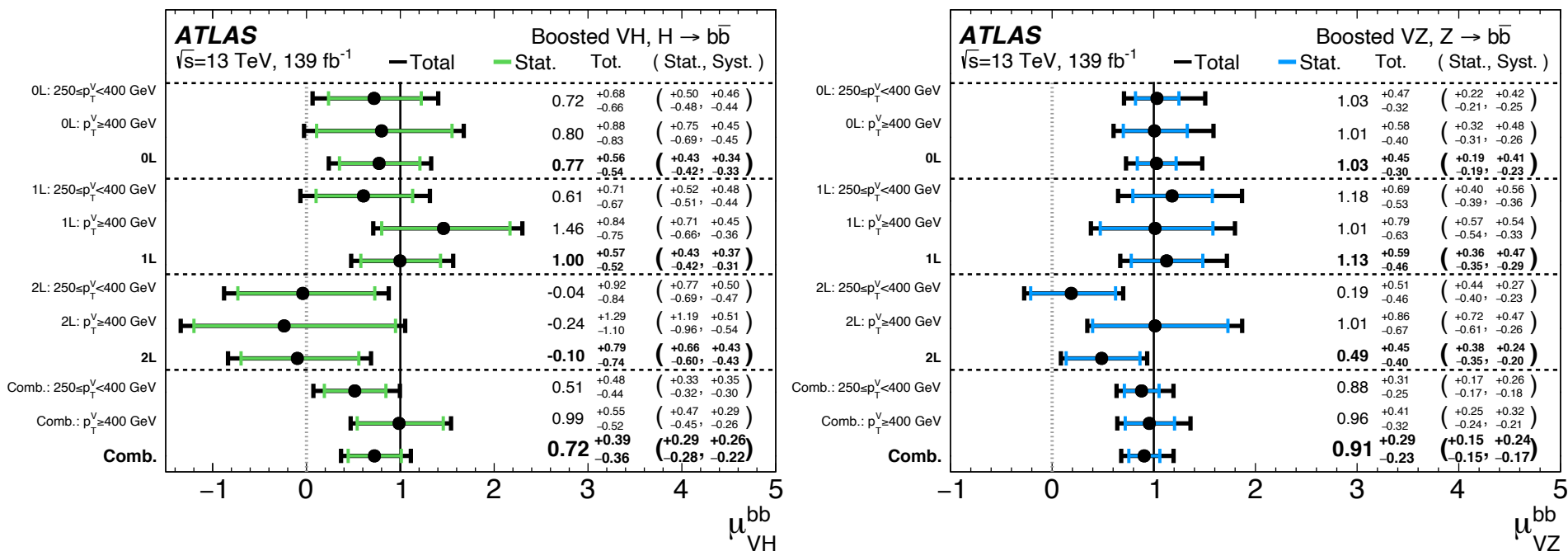
Postfit event yields: 1L

| Processes | $250 \text{ GeV} < p_T^V \leq 400 \text{ GeV}$ | | | $p_T^V > 400 \text{ GeV}$ | | |
|---------------|--|-----------------|-----------------|---------------------------|-----------------|-----------------|
| | HP SR | LP SR | CR | HP SR | LP SR | CR |
| $W + t$ | 64 ± 21 | 160 ± 75 | 73 ± 30 | 16.4 ± 7.3 | 53 ± 42 | 21 ± 15 |
| other $t + X$ | 1.92 ± 0.48 | 16.3 ± 0.3 | 21.9 ± 6.2 | 0.13 ± 0.01 | 1.70 ± 0.06 | 4.0 ± 1.4 |
| $t\bar{t}$ | 235 ± 30 | 1190 ± 76 | 1758 ± 58 | 50.9 ± 7.3 | 227 ± 24 | 341 ± 25 |
| VZ | 35.9 ± 8.9 | 56 ± 14 | 5.0 ± 1.4 | 8.63 ± 2.3 | 20.0 ± 5.3 | 2.61 ± 0.84 |
| WW | - | 6.8 ± 1.6 | 0.27 ± 0.01 | 0.15 ± 0.02 | 4.68 ± 1.32 | 0.93 ± 0.03 |
| $W+HF$ | 265 ± 28 | 617 ± 64 | 60 ± 22 | 91 ± 12 | 239 ± 30 | 26.6 ± 9.8 |
| $W + cl$ | 7.33 ± 2.9 | 13.8 ± 5.7 | 2.10 ± 0.04 | 6.2 ± 2.5 | 10.2 ± 4.1 | 0.63 ± 0.02 |
| $W + l$ | 3.0 ± 1.5 | 5.7 ± 3.4 | 0.65 ± 0.01 | 2.2 ± 1.4 | 7.7 ± 5.0 | 0.31 ± 0.01 |
| $Z+HF$ | 10.2 ± 1.2 | 24.6 ± 2.5 | 3.45 ± 0.41 | 2.12 ± 0.30 | 6.56 ± 0.79 | 0.98 ± 0.12 |
| $Z + cl$ | - | 0.75 ± 0.02 | - | - | 0.33 ± 0.01 | - |
| $Z + l$ | - | 0.49 ± 0.01 | - | 0.30 ± 0.19 | 0.23 ± 0.01 | - |
| MultiJet | 17.0 ± 8.9 | 44 ± 23 | 22 ± 11 | 7.8 ± 4.5 | 22 ± 13 | 7.9 ± 4.0 |
| Signal | 24 ± 12 | 18.0 ± 9.3 | 0.86 ± 0.45 | 7.8 ± 4.0 | 7.5 ± 3.9 | 0.39 ± 0.20 |
| Background | 640 ± 26 | 2136 ± 44 | 1947 ± 43 | 186 ± 11 | 592 ± 21 | 406 ± 18 |
| data | 668 | 2161 | 1946 | 185 | 597 | 410 |

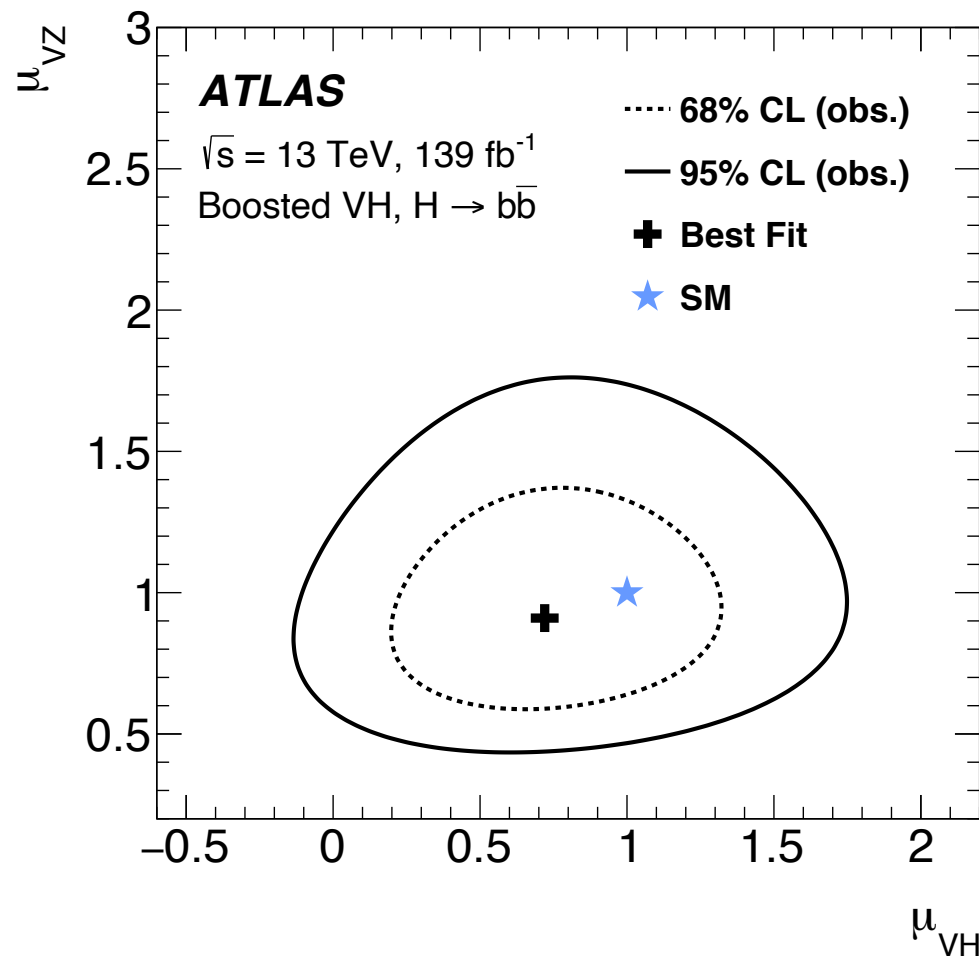
Postfit event yields: 2L

| Processes | $250 \text{ GeV} < p_T^V \leq 400 \text{ GeV}$ | $p_T^V > 400 \text{ GeV}$ |
|---------------|--|---------------------------|
| | SR | SR |
| $W + t$ | 1.28 ± 0.39 | - |
| $t\bar{t}$ | 1.64 ± 0.35 | 0.45 ± 0.10 |
| VZ | 19.9 ± 4.9 | 7.5 ± 2.1 |
| $W+\text{HF}$ | 0.41 ± 0.07 | 0.07 ± 0.01 |
| $Z+\text{HF}$ | 151 ± 13 | 57.2 ± 5.8 |
| $Z + cl$ | 2.20 ± 0.91 | 1.80 ± 0.76 |
| $Z + l$ | 0.94 ± 0.67 | 1.01 ± 0.67 |
| Signal | 7.6 ± 3.9 | 2.8 ± 1.4 |
| Background | 177 ± 12 | 68.0 ± 5.6 |
| data | 179 | 73 |

Multi POI fits: μ_{VH} and μ_{VZ}

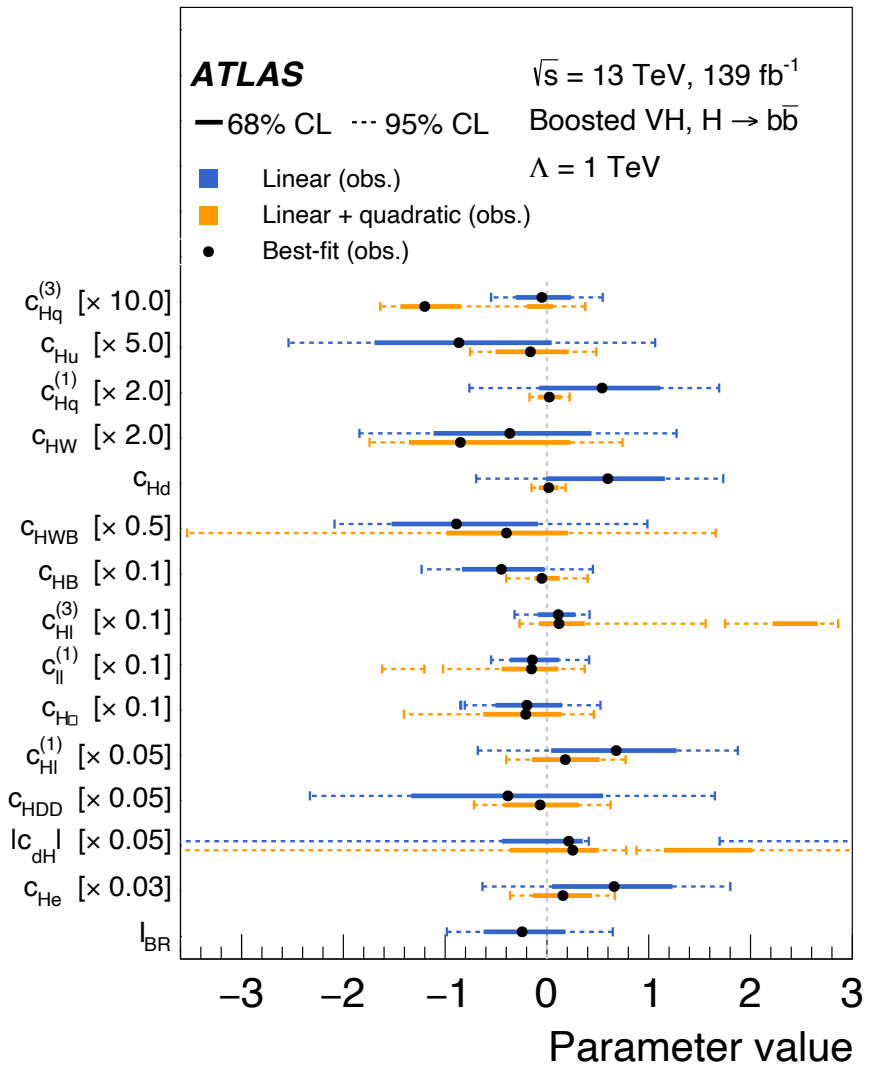


Measured CL μ_{VH} and μ_{VZ}



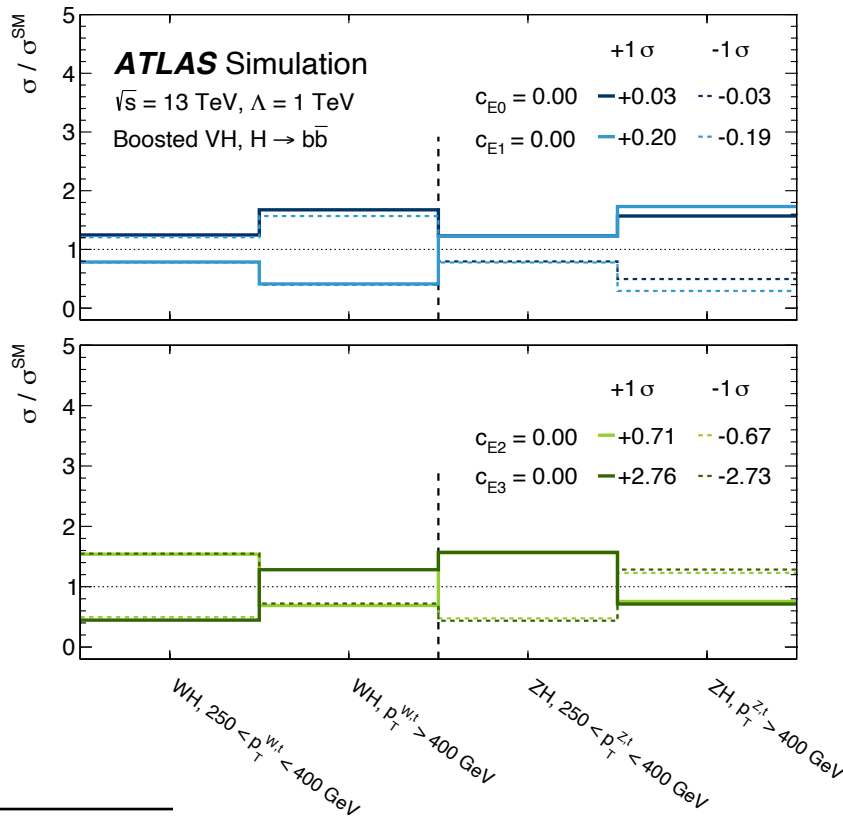
EFT interpretation results

| Coefficient | Operator |
|----------------|--|
| c_H | $(H^\dagger H)(H^\dagger H)$ |
| c_{HDD} | $(H^\dagger D^\mu H)^*(H^\dagger D_\mu H)$ |
| $ c_{dH} $ | $(H^\dagger H)(\bar{q}_p d_r H)$ |
| c_{HW} | $H^\dagger H W_{\mu\nu}^I W^{I\mu\nu}$ |
| c_{HB} | $H^\dagger H B_{\mu\nu} B^{\mu\nu}$ |
| c_{HWB} | $H^\dagger \tau^I H W_{\mu\nu}^I B^{\mu\nu}$ |
| $c_{Hl}^{(1)}$ | $H^\dagger i \overleftrightarrow{D}_\mu H (\bar{l}_p \gamma^\mu l_r)$ |
| $c_{Hl}^{(3)}$ | $H^\dagger i \overleftrightarrow{D}_\mu^I H (\bar{l}_p \tau^I \gamma^\mu l_r)$ |
| $c_{He}^{(1)}$ | $H^\dagger i \overleftrightarrow{D}_\mu H (\bar{e}_p \gamma^\mu e_r)$ |
| $c_{Hq}^{(1)}$ | $H^\dagger i \overleftrightarrow{D}_\mu H (\bar{q}_p \gamma^\mu q_r)$ |
| $c_{Hq}^{(3)}$ | $H^\dagger i \overleftrightarrow{D}_\mu^I H (\bar{q}_p \tau^I \gamma^\mu q_r)$ |
| c_{Hu} | $H^\dagger i \overleftrightarrow{D}_\mu H (\bar{u}_p \gamma^\mu u_r)$ |
| c_{Hd} | $H^\dagger i \overleftrightarrow{D}_\mu H (\bar{d}_p \gamma^\mu d_r)$ |
| $c_{ll}^{(1)}$ | $(\bar{l}_p \gamma_\mu l_r)(\bar{l}_s \gamma^\mu l_t)$ |



EFT results

| Coefficient | Expected | Observed |
|-------------|---------------------------|----------------------------|
| c_{EA} | $0.000^{+0.030}_{-0.027}$ | $-0.010^{+0.027}_{-0.025}$ |
| c_{EB} | $0.00^{+0.20}_{-0.19}$ | $-0.21^{+0.19}_{-0.20}$ |
| c_{EC} | $0.00^{+0.71}_{-0.67}$ | $-0.62^{+0.70}_{-0.66}$ |
| c_{ED} | $0.0^{+2.8}_{-2.7}$ | $0.4^{+2.8}_{-2.7}$ |



| Coefficient | Eigenvalue | Eigenvector combination |
|-------------|------------|--|
| c_{EA} | 1500.0 | $0.99 \cdot c_{Hq}^{(3)} + 0.11 \cdot c_{Hu}$ |
| c_{EB} | 26.9 | $0.82 \cdot c_{Hu} - 0.49 \cdot c_{Hq}^{(1)} - 0.24 \cdot c_{Hd} - 0.13 \cdot c_{Hq}^{(3)}$ |
| c_{EC} | 2.2 | $0.67 \cdot \mathcal{I}_{BR} + 0.66 \cdot c_{HW} + 0.18 \cdot c_{Hq}^{(1)} - 0.16 \cdot c_{Hl}^{(3)} + 0.14 \cdot c_{HWB} + 0.12 \cdot c_{ll}^{(1)}$ |
| c_{ED} | 0.1 | $0.70 \cdot c_{Hq}^{(1)} + 0.52 \cdot c_{HWB} + 0.27 \cdot c_{Hu} - 0.27 \cdot c_{HW} - 0.24 \cdot c_{Hd} + 0.13 \cdot c_{HB}$ |